



# CHORUS

This is the accepted manuscript made available via CHORUS. The article has been published as:

## Ground and excited $^1S$ states of the beryllium atom

István Hornyák, Ludwik Adamowicz, and Sergiy Bubin

Phys. Rev. A **100**, 032504 — Published 4 September 2019

DOI: [10.1103/PhysRevA.100.032504](https://doi.org/10.1103/PhysRevA.100.032504)

# Ground and excited $^1S$ -states of the beryllium atom

István Hornyák,<sup>1,\*</sup> Ludwik Adamowicz,<sup>2,3,†</sup> and Sergiy Bubín<sup>1,‡</sup>

<sup>1</sup>*Department of Physics, School of Science and Technology,  
Nazarbayev University, Astana 010000, Kazakhstan*

<sup>2</sup>*Department of Chemistry and Biochemistry, University of Arizona, Tucson, Arizona 85721, USA*

<sup>3</sup>*Department of Physics, University of Arizona, Tucson, Arizona 85721, USA*

Benchmark calculations of the total and transition energies of the four lowest  $^1S$  states of the beryllium atom are performed. The computational approach is based on variational calculations with finite mass of the nucleus. All-particle explicitly correlated Gaussian (ECG) functions are used to expand the total non-Born–Oppenheimer nonrelativistic wave functions and the ECG exponential parameters are optimized using the standard variational method. The leading relativistic and quantum electrodynamics energy corrections are calculated using the first-order perturbation theory. A comparison of the experimental transition frequencies with the ones calculated in this work shows an excellent agreement. The deviations of  $0.02 - 0.09 \text{ cm}^{-1}$  are well within the estimated error limits for the experimental values.

## I. INTRODUCTION

The purpose of the present work is to demonstrate the efficiency of the all-electron explicitly correlated Gaussian (ECG) functions in variational calculations of ground and excited atomic states and obtain highly accurate, benchmark results for one of the most heavily used workbenches of the electronic structure theory and the experiment [1] – the beryllium atom. In this work we consider the ground and the lowest three excited  $^1S$  states of Be. The common wisdom is that, due to quadratic dependency of the Gaussian exponent on the inter-particle (electron-electron and electron-nucleus) distances, the ECGs are inefficient in representing the long-distance behavior of the wave function and the electron-nucleus and electron-electron cusps being described by the Kato conditions. In this work we show that slowly growing the basis set for each of the considered states and thoroughly optimizing of the Gaussian exponential parameters with a procedure that employs the analytical energy gradient determined with respect to these parameters can produce results which are very close to exact.

Quantum-mechanical calculations of the beryllium atom have a long history of successive improvements [2–28]. Recently there have been some works where the accuracy of the nonrelativistic energies of the lowest few bound states approaches or exceeds one part per billion [27, 29–31]. Most of these ultra-high accuracy calculations have been performed using ECGs. The ECG-expanded wave functions obtained variationally at the nonrelativistic level have been used to calculate the leading relativistic and QED (quantum electrodynamics) corrections. As these corrections are represented by highly singular operators, it is important that the wave functions used in their calculations are very accurate. There

are two main differences between the way our atomic ECG calculations are performed and the calculations performed by others [29, 30] which make our nonrelativistic wave functions potentially more accurate. Firstly, the nonrelativistic Hamiltonian used in our calculations explicitly depends on the finite nuclear mass (FNM). Thus, the FNM effects are included non-perturbatively in both the total nonrelativistic energy and the wave function. These effects are also explicitly included in the relativistic and QED corrections. Secondly, the use of the energy gradient significantly accelerates the convergence of the variational minimization of the nonrelativistic energy and allows for achieving very accurate results much faster than when the gradient is not used.

## II. FORMALISM

In our recent work on ground and excited  $^1S$  state of  $^{10}\text{B}$  and  $^{11}\text{B}$  boron isotopes [32], a computational approach for calculating such states, which was an improvement from the approach presented earlier [31] in the work on the lowest  $^1S$  states of  $^9\text{Be}$ , was described. Some important refinements are implemented in the new approach. They include the Araki–Sucher and Kabir–Salpeter terms, which appear in the QED correction. The terms are implemented within the non-Born–Oppenheimer (non-BO) approach. Also, the computer code is made more efficient in terms of its parallel performance. Moreover, the regularization approach (commonly called “drachmanization” [33, 34]) is implemented in the calculation of certain expectation values, including those used in the calculations of relativistic and QED corrections, using the non-BO wave functions. The new approach allows to extend the range of the calculations to five-electron atom with a similar accuracy as achieved before in our Be calculations performed in 2007. In present work, the new upgraded approach is applied to recalculate the four lowest  $^1S$  states of the beryllium and much improved results are obtained.

<sup>9</sup>Be atom is a five-particle system with four elec-

---

\* istvan.hornyak@nu.edu.kz

† ludwik@email.arizona.edu

‡ sergiy.bubin@nu.edu.kz

trons and a nucleus. We start by writing the complete nonrelativistic Hamiltonian,  $H$ , of this system using a set of 15 laboratory-frame Cartesian coordinates,  $(\mathbf{R}_i, i = 1, \dots, 5)$ , where  $\mathbf{R}_i$  is the position vector of particle  $i$  in the laboratory Cartesian coordinate system). After separating out the motion of the center of mass, the five-particle problem is reduced to an effective four-particle problem. The separation is achieved by transforming  $H$  from the laboratory coordinate system to a new set of Cartesian coordinates whose first three  $(\mathbf{r}_0)$  are the center of mass coordinates in the laboratory coordinate frame and the remaining  $15 - 3 = 12$  are so-called internal coordinates  $(\mathbf{r}, i = 1, \dots, 4)$ . The center of the internal coordinate system is placed at the nucleus and vector  $\mathbf{r}_i$  is the position vector of particle  $i + 1$  (electron) with respect to particle 1 (the nucleus). The separation is rigorous and results in  $H$  splitting into the Hamiltonian representing the kinetic energy of the center-of-mass motion and the internal nonrelativistic Hamiltonian,  $H_{\text{nr}}$ , which for the beryllium atom in atomic units (a.u.) is:

$$H_{\text{nr}} = -\frac{1}{2} \left( \sum_{i=1}^4 \frac{1}{\mu_i} \nabla_{\mathbf{r}_i}^2 + \sum_{i=1}^4 \sum_{j \neq i}^4 \frac{1}{m_0} \nabla_{\mathbf{r}_i} \cdot \nabla_{\mathbf{r}_j} \right) + \sum_{i=1}^4 \frac{q_0 q_i}{r_i} + \sum_{i=1}^4 \sum_{j < i}^4 \frac{q_i q_j}{r_{ij}}, \quad (1)$$

where, in atomic units,  $q_0 = 4$  is the charge of the nucleus,  $q_1 = q_2 = q_3 = q_4 = -1$  are the charges of the electrons,  $m_0 = 16424.2055$  is the mass of the  $^9\text{Be}$  nucleus,  $\mu_i = m_0 m_i / (m_0 + m_i)$  are the reduced electron masses with  $m_1 = m_2 = m_3 = m_4 = 1$ . The position vectors of the electrons with respect to the nucleus are  $\mathbf{r}_i$ , where  $i = 1, 2, 3$ , and 4,  $r_i$  are their lengths, and the distances between the electrons are  $r_{ij} = |\mathbf{r}_j - \mathbf{r}_i|$ . The effect of the finite nuclear mass is represented by the mass-polarization term and the presence of the reduced masses in the kinetic-energy operator. Hamiltonian (1) represents the total nonrelativistic energy of a system of four particles that can be called pseudo-particles, as, while their charges are the charges of the electrons, their masses are not electron masses but reduced masses.

In this work, the following explicitly correlated all-particles Gaussian functions (ECGs) are used for expanding the spatial parts of the wave functions of the  $^1S$  states of  $^9\text{Be}$ :

$$\phi_k = \exp[-\mathbf{r}' (L_k L_k' \otimes I_3) \mathbf{r}], \quad (2)$$

where  $\otimes$  denotes the Kronecker product,  $\mathbf{r}$  is a  $12 \times 1$  vector of the internal Cartesian coordinates of the pseudo-particles,  $L_k$  is a lower triangular matrix of nonlinear variation parameters ( $4 \times 4$  matrix), and  $I_3$  is the  $3 \times 3$  identity matrix. Square integrability of the Gaussian is ensured by the Cholesky-factored form of the  $L_k L_k'$  product.

In the nonrelativistic calculations performed in this work we use the standard variational method and each

state is calculated separately and independently. The nonlinear parameters (i.e., the matrix elements of  $L_k$ ) and the linear coefficients in the expansion of the wave function in terms of ECGs are determined by performing minimization of the nonrelativistic total internal energy. This minimization is a multistep approach that employs the analytic gradient of the energy determine with respect to the ECG nonlinear parameters [35]. The use of the gradient in the minimization considerably reduces the computational cost because the minimization process is significantly accelerated [36, 37].

Even though the optimization of the ECG basis set and the generation of the wave functions for each state is carried out in separate calculations, the procedure used makes the calculated wave function orthogonal to the wave functions of all lower states expressed in terms of the basis set used in the calculation. Thus, all total energies obtained in this work are strict upper bounds to the corresponding exact energy values. However, the final wave functions obtained for different states are not, strictly speaking, exactly orthogonal to each other, as they are obtained in different basis sets generated for each state in separate calculations. As the total energies of the four considered states are uniformly very well converged, the deviation from the exact orthogonality should be very small.

In the present calculations we use the spin-free formalism to ensure the correct permutational symmetry properties of the wave function. In this formalism, an appropriate symmetry projector is constructed and applied to each basis function (2). In constructing the symmetry projector the standard procedure involving Young operators (as described, for example, in Ref. [38]) is used. In the case of the  $^1S$  states of beryllium, the permutation operator can be chosen to be  $(1 - P_{24})(1 - P_{35})(1 + P_{23})(1 + P_{45})$ , where  $P_{ij}$  denotes the permutation of the spatial coordinates of the  $i$ th and  $j$ th particle (particle 1 is the nucleus). The above projector yields  $4! = 24$  terms for each matrix element of the overlap, Hamiltonian and all other relevant operators.

The most practical approach to account for relativistic and QED effects for light atoms is to expand the total energy in powers of the fine structure constant,  $\alpha$  [39, 40]:

$$E_{\text{tot}} = E_{\text{nr}} + \alpha^2 E_{\text{rel}}^{(2)} + \alpha^3 E_{\text{QED}}^{(3)} + \alpha^4 E_{\text{HQED}}^{(4)} + \dots, \quad (3)$$

where  $E_{\text{nr}}$  is an eigenvalue of the nonrelativistic Hamiltonian (1),  $\alpha^2 E_{\text{rel}}^{(3)}$  includes the leading relativistic correction, and the leading and higher-order QED corrections are represented by  $\alpha^3 E_{\text{QED}}^{(3)}$  and  $\alpha^4 E_{\text{HQED}}^{(4)}$ . In calculating the relativistic effects we use the Dirac-Breit Hamiltonian in the Pauli approximation [41, 42] transformed from the laboratory coordinates to the internal coordinates. For the  $^1S$  states considered in the present work,  $H_{\text{rel}}$  includes the mass-velocity  $H_{\text{MV}}$ , Darwin  $H_{\text{D}}$ , orbit-orbit  $H_{\text{OO}}$ , and spin-spin  $H_{\text{SS}}$  terms:

$$H_{\text{rel}} = H_{\text{MV}} + H_{\text{D}} + H_{\text{OO}} + H_{\text{SS}}. \quad (4)$$

Their explicit form is given by [35]

$$H_{\text{MV}} = -\frac{1}{8} \left[ \frac{1}{m_0^3} \left( \sum_{i=1}^4 \nabla_{\mathbf{r}_i} \right)^4 + \sum_{i=1}^4 \frac{1}{m_i^3} \nabla_{\mathbf{r}_i}^4 \right], \quad (5)$$

$$H_{\text{D}} = -\frac{\pi}{2} \left( \sum_{i=1}^4 \frac{q_0 q_i}{m_i^2} \delta(\mathbf{r}_i) + \sum_{\substack{i,j=1 \\ j \neq i}}^4 \frac{q_i q_j}{m_i^2} \delta(\mathbf{r}_{ij}) \right), \quad (6)$$

$$\begin{aligned} H_{\text{OO}} = & \\ & -\frac{1}{2} \sum_{i=1}^4 \frac{q_0 q_i}{m_0 m_i} \left( \frac{1}{r_i} \nabla_{\mathbf{r}_i} \cdot \nabla_{\mathbf{r}_i} + \frac{1}{r_i^3} \mathbf{r}_i \cdot (\mathbf{r}_i \cdot \nabla_{\mathbf{r}_i}) \nabla_{\mathbf{r}_i} \right) \quad (7) \\ & -\frac{1}{2} \sum_{\substack{i,j=1 \\ j \neq i}}^4 \frac{q_0 q_i}{m_0 m_i} \left( \frac{1}{r_i} \nabla_{\mathbf{r}_i} \cdot \nabla_{\mathbf{r}_j} + \frac{1}{r_i^3} \mathbf{r}_i \cdot (\mathbf{r}_i \cdot \nabla_{\mathbf{r}_i}) \nabla_{\mathbf{r}_j} \right) \\ & + \frac{1}{2} \sum_{\substack{i,j=1 \\ j > i}}^4 \frac{q_i q_j}{m_i m_j} \left( \frac{1}{r_{ij}} \nabla_{\mathbf{r}_i} \cdot \nabla_{\mathbf{r}_j} + \frac{1}{r_{ij}^3} \mathbf{r}_{ij} \cdot (\mathbf{r}_{ij} \cdot \nabla_{\mathbf{r}_i}) \nabla_{\mathbf{r}_j} \right), \end{aligned}$$

and

$$H_{\text{SS}} = -\frac{8\pi}{3} \sum_{\substack{i,j=1 \\ j > i}}^4 \frac{q_i q_j}{m_i m_j} (\mathbf{s}_i \cdot \mathbf{s}_j) \delta(\mathbf{r}_{ij}), \quad (8)$$

where  $\delta(\mathbf{r})$  is the Dirac delta function and  $\mathbf{s}_i$  are spin operators for individual electrons. For the states considered in this work  $\mathbf{s}_i \cdot \mathbf{s}_j = -3/4$ .

The leading QED correction for the beryllium atom that accounts for the two-photon exchange, the vacuum polarization, and the electron self-energy effects are expressed as:

$$\begin{aligned} H_{\text{QED}} = & \sum_{\substack{i,j=1 \\ j > i}}^4 \left[ \left( \frac{164}{15} + \frac{14}{3} \ln \alpha \right) \delta(\mathbf{r}_{ij}) - \frac{7}{6\pi} P(r_{ij}^{-3}) \right] \\ & + \sum_{i=1}^4 \left( \frac{19}{30} - 2 \ln \alpha - \ln k_0 \right) \frac{4q_0}{3} \delta(\mathbf{r}_i). \quad (9) \end{aligned}$$

Here the first sum represents the Araki-Sucher term [43–47], while the expectation value of  $P(r_{ij}^{-3})$  is defined as:

$$\langle P(r_{ij}^{-3}) \rangle = \lim_{a \rightarrow 0} \langle r_{ij}^{-3} \Theta(r_{ij} - a) + 4\pi(\gamma + \ln a) \delta(\mathbf{r}_{ij}) \rangle, \quad (10)$$

where  $\Theta$  is the Heaviside step function and  $\gamma = 0.5772\dots$  is the Euler–Mascheroni constant. The numerical values of the conversion factor from a Hartree to a wavenumber and of the fine structure constant used in present work are:  $1\text{hartree} = 2.194\,746\,313\,705 \times 10^5 \text{ cm}^{-1}$  and  $\alpha = 7.297\,352\,537\,6 \times 10^{-3}$ , respectively. In the present calculations, we use the values of the Bethe logarithm,  $\ln k_0$ , which are presented in Table I. The values were

TABLE I. The Bethe logarithms for the lowest four  $^1S$  states of  $^9\text{Be}$  taken from Ref. [31]. All values are in atomic units.

State	$\ln k_0$
$2^1S$	5.75035
$3^1S$	5.75129
$4^1S$	5.75121
$5^1S$	5.75049

calculated in a previous work [31]. The HQED correction is calculated using the following approximate formula developed by Pachucki *et al.* [22, 48]:

$$H_{\text{HQED}} = \pi q_0^2 \left( \frac{427}{96} - 2 \ln 2 \right) \sum_{i=1}^4 \delta(\mathbf{r}_i). \quad (11)$$

It corresponds to the dominant part of the so-called one-loop term. The expectation values of the  $H_{\text{QED}}$  and  $H_{\text{HQED}}$  Hamiltonians are calculated with infinite nuclear mass (INM) wave functions, because these Hamiltonians are only valid for an infinite nuclear mass.

### III. RESULTS

In the first step of the present calculations the ECG basis set is grown up to the size of 7000 for each state using the variational method and the internal Hamiltonian, Eq. (1), that represents the total internal non-relativistic energy of  $^9\text{Be}$ . Our goal is to obtain the most converged energies possible using fewest basis functions. Achieving the goal has required several months of continuous calculations. The end results are the best (lowest) nonrelativistic variational energies ever obtained in the literature for all four lowest  $^1S$  states of the beryllium. It is remarkable that only 7000 ECGs are used for each state, which is fewer than in our previous work [31], where we generated basis sets of 10000 ECGs for the same states. At the same time the accuracy of the nonrelativistic energies are increased by nearly two and one order of magnitude for the ground and third excited state, respectively. All calculations are performed using 80-bit extended precision arithmetic.

Once the basis sets for the considered states are generated, they are used to perform calculations for the beryllium atom with infinite nuclear mass (INM),  $^\infty\text{Be}$ . This is done to make a direct comparison with the best literature energies obtained in calculations, where in the first step the INM non-relativistic energy (i.e. the energy of  $^\infty\text{Be}$ ) is obtained for each state and the corrections due the finite nuclear mass are calculated using the perturbation theory. For example, this type of approach was used in recent calculations of  $2^1S$ ,  $3^1S$ , and  $2^1P$  states of beryllium [29]. A comparison of the ground state nonrelativistic energies for  $^\infty\text{Be}$  obtained with various theoretical methods is given in table II. This table illustrates the

TABLE II. Comparison of the ground state nonrelativistic energies of  ${}^{\infty}\text{Be}$  obtained with various theoretical methods: PDVM (poly-deter variational method with exponential functions), CI (configuration interaction method), MBPT (many-body perturbation theory), Hy (Hylleraas-type functions), Hy-CI (Hylleraas-CI), MCHF (multi-configuration Hartree-Fock method), EE (estimated exact), ECG (explicitly correlated Gaussian functions), DMC (Diffusion Monte Carlo), LSE-FICI (Local Schrödinger Equation over Free Iterative-Complement-Interaction wave function), ECFCC (explicitly correlated factorizable coupled-cluster method). Some of the quoted values include extrapolation to the infinite basis set.

Year	Reference	Method	Energy (a.u.)
1953	Boys and Lennard-Jones	[2] PDVM	-14.637
1960	Watson	[3] CI	-14.657 40
1961	Weiss	[4] CI	-14.660 90
1963	Kelly	[5] MBPT	-14.663 11
1967	Szasz and Byrnes	[6] Hy	-14.656 5
1968	Gentner and Burke	[7] Hy	-14.657 9
1968	Bunge	[8] CI	-14.664 19
1971	Sims and Hagstrom	[9] Hy-CI	-14.666 547
1974	Fischer and Saxena	[10] MCHF	-14.665 87
1976	Bunge	[11] CI	-14.666 902
1991	Mårtensson-Pendrill <i>et. al.</i>	[14] MCHF	-14.667 37
1991	Davidson <i>et. al.</i>	[15] EE	-14.667 36
1993	Fischer	[16] MCHF	-14.667 113
1993	Chakravorty <i>et. al.</i>	[17] EE	-14.667 36
1995	Komasa <i>et. al.</i>	[18] ECG	-14.667 360(2)
1997	Jitrik and Bunge	[19] CI	-14.667 275 57
1998	Büsse and Lüchow	[20] Hy	-14.667 354 7
2004	Pachucki and Komasa	[22] ECG	-14.667 355 7(1)
2006	Pachucki and Komasa	[23] ECG	-14.667 355 748
2007	Nakatsuji <i>et. al.</i>	[49] LSE-ICI	-14.667 300
2009	Stanke <i>et. al.</i>	[31] ECG	-14.667 356 486
2010	Verdebout <i>et. al.</i>	[24] MCHF	-14.667 114 52
2010	Bunge	[25] CI	-14.667 355(1)
2011	Seth <i>et. al.</i>	[50] DMC	-14.667 306(7)
2011	Sims and Hagstrom	[26] Hy-CI	-14.667 356 411
2013	Puchalski <i>et. al.</i>	[30] ECG	-14.667 356 498(3)
2014	Sims and Hagstrom	[27] Hy-CI	-14.667 356 407 951
2018	Przybytek and Lesiuk	[28] ECFCC	-14.667 351(6)
2019	Present work	ECG	-14.667 356 508(1)

progress made in the ground-state beryllium calculations over the last seven decades.

In table III the nonrelativistic energies and some key expectation values for the lowest four  $1S$  states of beryllium obtained in the present calculations are shown. These expectation values include the mass-velocity correction, the Dirac delta functions, the orbit-orbit correction, and the Araki-Sucher distribution denoted as:  $E_{\text{nr}}$ ,  $\langle \tilde{H}_{\text{MV}} \rangle$ ,  $\langle \tilde{\delta}(\mathbf{r}_i) \rangle$ ,  $\langle \tilde{\delta}(\mathbf{r}_{ij}) \rangle$ ,  $\langle H_{\text{OO}} \rangle$ , and  $\langle \mathcal{P}(1/r_{ij}^3) \rangle$ , respectively. The tilde in an expectation value denotes the fact that it was computed using the regularization in the spirit of works [33, 34]. Table III shows the convergence of the nonrelativistic energies and the expectation values of  ${}^9\text{Be}$  with the number of basis functions.

The nonrelativistic energies for states  $2^1S$  and  $3^1S$  can be compared with the values reported by Puchal-

ski *et al.* [29] and obtained by extrapolating their calculated results to infinite number of basis functions. For the ground ( $2^1S$ ) state their extrapolated value of  $-14.667\,356\,498(3)$  hartree is slightly higher than the result of  $-14.667\,356\,507$  hartree we obtain with 7000 ECGs and also slightly higher than our extrapolated value of  $-14.667\,356\,508(1)$  hartree, which suggests that somewhat too optimistic numerical error bar was used in that work. For the first excited ( $3^1S$ ) state, our best variational energy is  $-14.418\,240\,364$  hartree and the extrapolated value is  $-14.418\,240\,368(2)$ , while the extrapolated value in [29] is  $-14.418\,240\,37(5)$ . It is also interesting to compare the present nonrelativistic energies obtained with 7000 ECGs with our previous results obtained with 10000 ECGs [31]. This comparison shows that the strategy used for the optimization of the nonlinear Gaussian parameters has dramatic effect on the number of functions in the basis set and on the final energy. The total nonrelativistic variational energies of  ${}^9\text{Be}$  obtained in the present work for all four considered states are noticeably lower than the previous energies obtained with 10000 ECGs. The energy improvement increases with the level of excitation. For the ground  $2^1S$  state our present  ${}^9\text{Be}$  variational energy is  $-14.666\,435\,525$  hartree while the previous energy was  $-14.666\,435\,504$  hartree. For the next three states the comparison is as follows: for the  $3^1S$  state  $-14.417\,335\,139$  (present) vs.  $-14.417\,335\,103$  hartree (previous), for the  $4^1S$  state  $-14.369\,185\,506$  vs.  $-14.369\,185\,452$  hartree, and for the  $5^1S$  state  $-14.350\,610\,346$  vs.  $-14.350\,610\,414$  hartree. The comparison shows that by investing more effort into the optimization of the ECG nonlinear parameters one gets much more compact basis set and an improved energy.

Table IV shows the expectation values of some powers of the interparticle distances:  $\langle r_i^p \rangle$  and  $\langle r_{ij}^p \rangle$ ,  $p = -2, -1, 1, 2$ , for the lowest four  $1S$  states of the  ${}^9\text{Be}$  isotope of the beryllium atom. The results obtained for different basis-set sizes allow for assessing the convergence of the expectation values. The results obtained with an infinite nuclear mass are also shown. Looking at the table, one may find interesting that the average nucleus-electron distance and the average electron-electron distance for all four states decreases slightly when the nuclear mass changes from the finite value to infinity.

In table V we show the transition energy values calculated using the infinite-nuclear-mass and finite-nuclear-mass nonrelativistic energies, and with the energies that include the relativistic and QED corrections. In the table, the transition energies derived from experimental data are also shown. The latter are taken from the paper of Kramida and Martin [51]. The experimental data was originally obtained by Johansson [52]. The accuracy of the experimental results can be estimated based on Johansson's statement, which can be found in his paper, that the error in his transition energy measurement should be less than  $0.05\text{ cm}^{-1}$ . As each experimental transition included in Table V is determined indirectly



TABLE III. Nonrelativistic energies and some key expectation values for the lowest four  $1S$  states of beryllium. All values are in atomic units.

State	Isotope	Basis size	$E_{nr}$	$\langle \tilde{H}_{MV} \rangle$	$\langle \tilde{\delta}(\mathbf{r}_i) \rangle$	$\langle \tilde{\delta}(\mathbf{r}_{ij}) \rangle$	$\langle H_{OO} \rangle$	$\langle \mathcal{P}(1/r_{ij}^3) \rangle$
$2^1S$	${}^9\text{Be}$	1000	-14.666434601	-270.637676	8.84061391	0.267505901	-0.91846434	
		2000	-14.666435372	-270.637204	8.84061646	0.267506202	-0.91846269	
		3000	-14.666435492	-270.636812	8.84061715	0.267506263	-0.91846173	
		4000	-14.666435516	-270.636754	8.84061727	0.267506276	-0.91846164	
		5000	-14.666435522	-270.636665	8.84061732	0.267506281	-0.91846160	
		6000	-14.666435524	-270.636661	8.84061734	0.267506283	-0.91846159	
		7000	-14.666435525	-270.636610	8.84061734	0.267506284	-0.91846158	
		$\infty$	-14.666435526(1)					
	${}^\infty\text{Be}$	7000	-14.667356507	-270.703579	8.84225164	0.267550915	-0.89182362	-1.22252
		$\infty$	-14.667356508(1)					
$3^1S$	${}^9\text{Be}$	1000	-14.417329757	-268.476884	8.78034563	0.263818856	-0.92655400	
		2000	-14.417334680	-268.476217	8.78037477	0.263820128	-0.92654211	
		3000	-14.417335008	-268.475616	8.78037595	0.263820283	-0.92654023	
		4000	-14.417335102	-268.475342	8.78037656	0.263820334	-0.92653974	
		5000	-14.417335126	-268.475219	8.78037666	0.263820352	-0.92653960	
		6000	-14.417335135	-268.474932	8.78037672	0.263820366	-0.92653944	
		7000	-14.417335139	-268.474926	8.78037676	0.263820371	-0.92653941	
		$\infty$	-14.417335143(2)					
	${}^\infty\text{Be}$	7000	-14.418240364	-268.541251	8.78199650	0.263864248	-0.90012821	-1.24822
		$\infty$	-14.418240368(2)					
$4^1S$	${}^9\text{Be}$	1000	-14.369172096	-268.321095	8.77620487	0.263506750	-0.93246815	
		2000	-14.369184708	-268.316753	8.77622461	0.263512300	-0.93234116	
		3000	-14.369185286	-268.316485	8.77622729	0.263512664	-0.93233897	
		4000	-14.369185438	-268.315943	8.77622809	0.263512761	-0.93233805	
		5000	-14.369185482	-268.315919	8.77622832	0.263512786	-0.93233795	
		6000	-14.369185498	-268.315837	8.77622842	0.263512800	-0.93233785	
		7000	-14.369185506	-268.315685	8.77622847	0.263512813	-0.93233771	
		$\infty$	-14.369185514(4)					
	${}^\infty\text{Be}$	7000	-14.370087930	-268.381937	8.77784635	0.263556591	-0.90593865	-1.25516
		$\infty$	-14.370087938(4)					
$5^1S$	${}^9\text{Be}$	1000	-14.350569397	-268.280889	8.77513779	0.263425561	-0.93411849	
		2000	-14.350608901	-268.273758	8.77515307	0.263429808	-0.93416778	
		3000	-14.350609974	-268.273927	8.77515866	0.263430294	-0.93416620	
		4000	-14.350610285	-268.273791	8.77516069	0.263430451	-0.93416515	
		5000	-14.350610369	-268.273701	8.77516129	0.263430505	-0.93416498	
		6000	-14.350610400	-268.273173	8.77516149	0.263430562	-0.93416442	
		7000	-14.350610414	-268.273164	8.77516159	0.263430571	-0.93416445	
		$\infty$	-14.350610428(7)					
	${}^\infty\text{Be}$	7000	-14.351511722	-268.339399	8.77677903	0.263474325	-0.90776818	-1.25659
		$\infty$	-14.351511736(7)					

from two  $mP \leftarrow nS$  transitions, it is reasonable to assume the experimental uncertainty to be about  $0.1 \text{ cm}^{-1}$  or less.

The nonlinear least-square fitting procedure is used to extrapolate the total energies to an infinite number of basis functions. The exponential fitting is used in the extrapolation. Based on the extrapolated energy values, the errors in the transition energies, shown in Table V, are estimated. It needs to be said, that, as the extrapolation

procedure is somewhat arbitrary, the errors shown in the table should be considered as approximations.

As one can see, the energies for the  $2^1S \leftarrow 3^1S$ ,  $3^1S \leftarrow 4^1S$  and  $4^1S \leftarrow 5^1S$  transitions calculated using the FNM nonrelativistic energies augmented with the relativistic and QED corrections differ from the experimental results by  $0.09$ ,  $0.02$ , and  $0.03 \text{ cm}^{-1}$ , respectively. This shows that the calculated expectation values are within the error limits of the experimental data.

TABLE IV. Expectation values  $\langle r_i^p \rangle$  and  $\langle r_{ij}^p \rangle$ , where  $p = -2, -1, 1, 2$ , for the lowest four  $1S$  states of beryllium atom. All values are in atomic units.

State	Isotope	Basis size	$\langle r_i^{-2} \rangle$	$\langle r_{ij}^{-2} \rangle$	$\langle r_i^{-1} \rangle$	$\langle r_{ij}^{-1} \rangle$	$\langle r_i \rangle$	$\langle r_{ij} \rangle$	$\langle r_i^2 \rangle$	$\langle r_{ij}^2 \rangle$
$2^1S$	$^9\text{Be}$	1000	14.39765189	1.589311227	2.1067072010	0.729074462277	1.49319387824	2.5454404750	4.062028723	8.809321702
		2000	14.39765577	1.589308531	2.1067072432	0.729074324545	1.49319455076	2.5454428641	4.062040691	8.809350957
		3000	14.39765683	1.589308311	2.1067073338	0.729074404565	1.49319434858	2.5454426866	4.062039998	8.809350617
		4000	14.39765701	1.589308237	2.1067073391	0.729074403675	1.49319435569	2.5454427397	4.062040236	8.809351322
		5000	14.39765708	1.589308204	2.1067073413	0.729074404502	1.49319435043	2.5454427402	4.062040246	8.809351388
		6000	14.39765710	1.589308196	2.1067073420	0.729074404678	1.49319434903	2.5454427412	4.062040252	8.809351415
		7000	14.39765711	1.589308188	2.1067073422	0.729074404661	1.49319434912	2.5454427435	4.062040262	8.809351446
	$^\infty\text{Be}$	7000	14.39943849	1.589480291	2.1068377887	0.729115267915	1.49310298993	2.5452913267	4.061541801	8.808305776
$3^1S$	$^9\text{Be}$	1000	14.26635128	1.502877062	2.0331763403	0.61603088210	2.823241920	5.075363293	20.725514629	42.25356629
		2000	14.26639361	1.502870731	2.0331806054	0.61603671663	2.823170388	5.075240002	20.725113846	42.25282679
		3000	14.26639532	1.502869458	2.0331806581	0.61603676964	2.823167552	5.075235830	20.725090246	42.25279413
		4000	14.26639618	1.502869066	2.0331806852	0.61603679331	2.823166810	5.075234818	20.725086925	42.25279221
		5000	14.26639633	1.502868939	2.0331806899	0.61603679799	2.823166547	5.075234408	20.725083447	42.25278649
		6000	14.26639642	1.502868839	2.0331806919	0.61603680016	2.823166449	5.075234258	20.725082415	42.25278483
		7000	14.26639647	1.502868815	2.0331806926	0.61603680057	2.823166426	5.075234235	20.725082562	42.25278545
	$^\infty\text{Be}$	7000	14.26815778	1.503030574	2.0333066736	0.61607100670	2.822996159	5.074929892	20.722602653	42.24773010
$4^1S$	$^9\text{Be}$	1000	14.25341579	1.48984661	2.0138355230	0.5805103147	4.93112377	9.2363628	79.554253	159.600833
		2000	14.25344649	1.48982585	2.0138464044	0.5805289692	4.92872683	9.2316386	79.461416	159.416180
		3000	14.25345032	1.48982352	2.0138465714	0.5805291242	4.92868998	9.2315709	79.460086	159.413611
		4000	14.25345145	1.48982273	2.0138466098	0.5805291528	4.92868295	9.2315580	79.459901	159.413253
		5000	14.25345179	1.48982257	2.0138466214	0.5805291644	4.92867959	9.2315517	79.459777	159.413009
		6000	14.25345192	1.48982248	2.0138466259	0.5805291692	4.92867848	9.2315496	79.459742	159.412941
		7000	14.25345200	1.48982239	2.0138466269	0.5805291698	4.92867799	9.2315487	79.459725	159.412907
	$^\infty\text{Be}$	7000	14.25521052	1.48998272	2.0139715224	0.5805614199	4.92837706	9.2309891	79.450069	159.393597
$5^1S$	$^9\text{Be}$	1000	14.24983864	1.48606196	2.0057906611	0.5652374272	7.80087032	14.9546366	223.08108	446.4884
		2000	14.24984692	1.48599598	2.0057984599	0.5652599224	7.79217445	14.9375539	222.64284	445.6122
		3000	14.24985479	1.48599266	2.0057987643	0.5652601302	7.79197416	14.9371638	222.62763	445.5819
		4000	14.24985760	1.48599130	2.0057988218	0.5652601301	7.79192566	14.9370704	222.62420	445.5751
		5000	14.24985840	1.48599096	2.0057988489	0.5652601552	7.79190685	14.9370338	222.62291	445.5725
		6000	14.24985868	1.48599060	2.0057988559	0.5652601577	7.79190091	14.9370223	222.62247	445.5716
		7000	14.24985883	1.48599055	2.0057988622	0.5652601649	7.79189756	14.9370158	222.62226	445.5712
	$^\infty\text{Be}$	7000	14.25161662	1.48615042	2.0059232455	0.5652914424	7.79143021	14.9361251	222.59546	445.5176

TABLE V. Transition energies between adjacent  $1S$  states of the  $^9\text{Be}$  atom computed using nonrelativistic energies with infinite nuclear mass (INM), and then gradually corrected by including finite nuclear mass (FNM), relativistic, and QED effects. As the QED and HQED Hamiltonians are only valid for INM, the corresponding energy corrections are calculated using the wave functions obtained in INM calculations. All values are in  $\text{cm}^{-1}$ .

Contributions included	Basis size	$2^1S \leftarrow 3^1S$	$3^1S \leftarrow 4^1S$	$4^1S \leftarrow 5^1S$
$\Delta E_{\text{nonrel}}$ (INM)	7000	54674.674	10568.238	4077.006
$\Delta E_{\text{nonrel}}$ (FNM)	7000	54671.215	10567.623	4076.761
$\Delta E_{\text{nonrel+rel}}$ (FNM)	7000	54677.881	10568.125	4076.900
$\Delta E_{\text{nonrel+rel+QED}}$ (FNM,INM)	7000	54677.375	10568.092	4076.901
$\Delta E_{\text{nonrel+rel+QED+HQED}}$ (FNM,INM)	7000	54677.352	10568.091	4076.901
$\Delta E_{\text{nonrel+rel+QED+HQED}}$ (FNM,INM)	$\infty$	54677.35(1)	10568.09(5)	4076.90(5)
Experiment		54677.26(10)	10568.07(10)	4076.87(10)

Nucleus-electron and electron-electron pair correlation functions are shown in Figures 1 and 2, respectively. The pair correlation functions are defined as:  $g_i(\mathbf{r}) = \langle \delta(\mathbf{r}_i - \mathbf{r}) \rangle$  for the nucleus and an electron, and by  $g_{ij}(\mathbf{r}) = \langle \delta(\mathbf{r}_{ij} - \mathbf{r}) \rangle$ , where  $i, j = 1, \dots, n$  and  $i \neq j$ , for a pair of electrons. The  $g_i(\mathbf{r})$  function represents the

probability density of particles 1 (the nucleus) and  $i + 1$  (an electron) to be found at distance  $r$  from each other.  $g_{ij}(\mathbf{r})$  represents the probability of particles  $i + 1$  and  $j + 1$  (two electrons) to be separated by distance  $r$ . So  $g_{ee} \equiv g_{ij}$  and  $g_{ne} \equiv g_i$ . Both correlation functions,  $g_{ne}(r)$  and  $g_{ee}(r)$ , are multiplied by  $4\pi r^2$  to convert them to

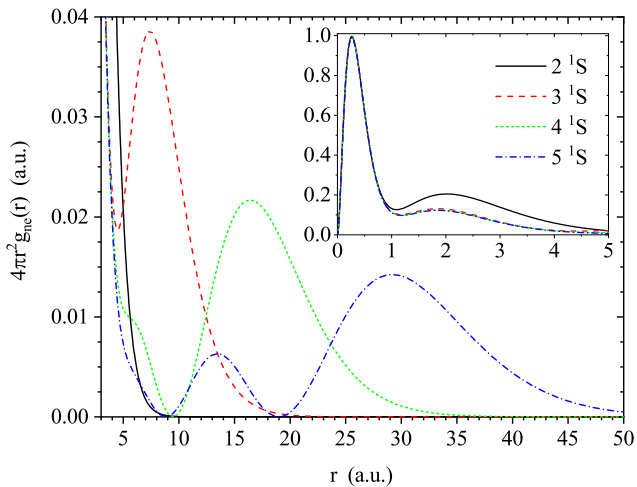


FIG. 1. Nucleus-electron pair correlation functions for the lowest four  $1S$  states of the beryllium atom.

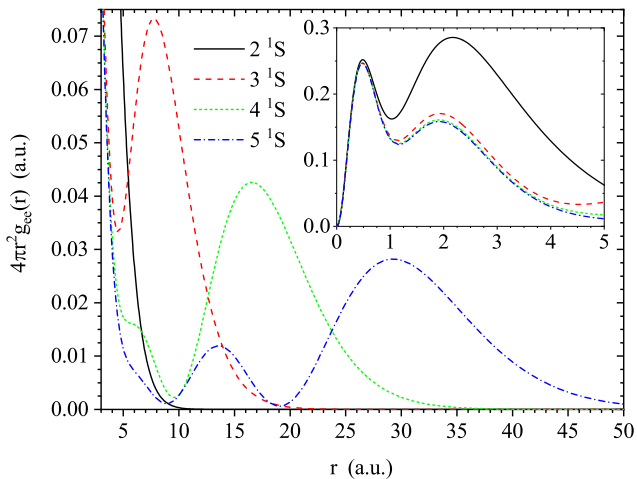


FIG. 2. Electron-electron pair correlation functions for the lowest four  $1S$  states of the beryllium atom.

properly normalized radial distributions. The  $1S$  states are spherically symmetric and so are the pair correlation functions.

The density of particle  $i$  in the center-of-mass (COM) coordinate frame is defined as  $\rho_i(\mathbf{r}) = \langle \delta(\mathbf{R}_i - \mathbf{r}_0 - \mathbf{r}) \rangle$ , where  $i = 1, \dots, N$  and  $\mathbf{r}_0$  is the position vector of the center of mass in the laboratory coordinate frame. The densities of the nucleus for the four considered states in the COM frame are shown in Figure 3, and the electron densities are shown in Figure 4. In both cases, the densities are multiplied by  $4\pi r^2$  to convert them to radial densities.

The COM-frame plots of the nucleus and electron density provide an interesting representation of the coupled motion of the nucleus and the electrons in the beryllium atom. This motion is a concerted motion of all particles

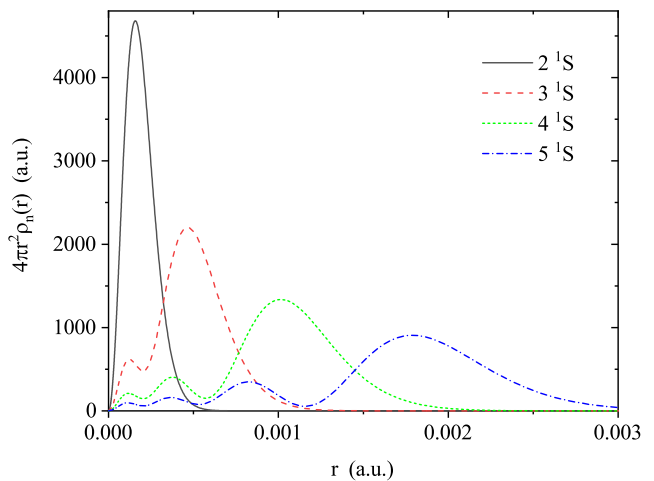


FIG. 3. The densities of the nucleus in the center-of-mass coordinate frame for the lowest four  $1S$  states of the beryllium atom.

forming the atom around center of mass of the system. Hence, if the atom is excited to increasingly higher state (from the ground  $1S$  state to the first, second, and third excited  $1S$  state), not only the average radius of the electronic density increases, which is manifested by increasing average value of the nucleus-electron average distance and by increasing diffuseness of the nucleus-electron pair density and COM-frame electron density, but also the electron density becomes more oscillatory. For example, there are four maxima in the COM-frame electron density of state  $5^1S$ , three maxima in the density of the  $4^1S$  state, etc. The same number of maxima can be seen in the corresponding COM-frame densities of the nucleus. The matching number of the maxima in the electronic and nuclear densities for a given state is understandable, because, only then the center-of-mass of the atom can remain immobile. However, due to much larger mass of the nucleus in comparison with the mass of the electrons, the characteristic scale of the nuclear motion around the center of mass is orders of magnitude smaller than the radius of the electronic motion. This is evident by comparing the scale of the horizontal axis is the plot of the COM-frame nuclear density (Figure 3) with the COM-frame electronic density (Figure 4).

#### IV. SUMMARY

This work features very accurate quantum-mechanical calculations of the four lowest  $1S$  states of the beryllium atom. The calculations are performed in the basis set of all-electron explicitly correlated Gaussian basis set using an approach where the finite mass of the nucleus is a part of the formalism from its first step, i.e. the variational calculation of the nonrelativistic energy and the corresponding wave function of the system (the finite-



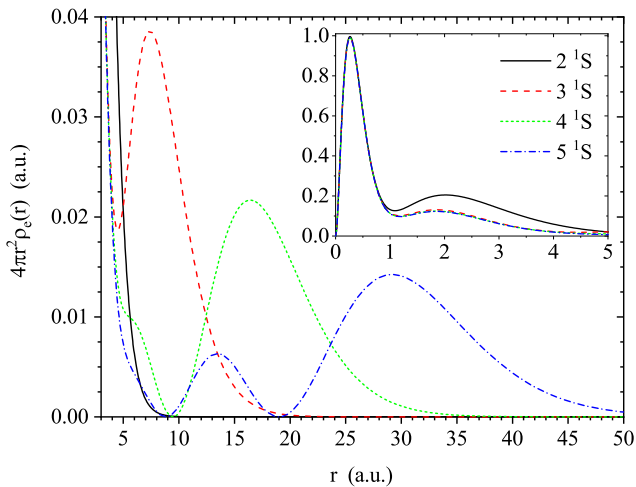


FIG. 4. The densities of electrons in the center-of-mass coordinate frame for the lowest four  $1S$  states of the beryllium atom.

nuclear-mass approach). The characterization of the four states includes the calculations of the leading relativistic and QED corrections which is done using the perturbation theory with the zeroth-order wave function being the FNM nonrelativistic wave function in the calculation of the relativistic corrections and the INM wave function in the calculation of the QED corrections. The total energies of the four states that include the nonrelativistic energy and the relativistic and QED corrections are used to calculate the transition energies between each two adjacent states. The calculated transition energies are compared with the most accurate experimental values and the two sets of results are shown to agree within  $0.02\text{-}0.09\text{ cm}^{-1}$ . The characterization of the four states also includes calculations of expectation values of pow-

ers of inter-particle distances and of operators representing terms appearing in the relativistic and QED corrections. We also compute and plot the nucleus-electron and electron-electron densities, as well as the densities of the nucleus and the electrons in the center-of-mass coordinate frame. The later densities describe the coupled nucleus-electron motion in the atom as a motion of two types of particles around the center of mass. The number of maxima in the COM-frame electron density for a particular state is, as expected, the same as the number of maxima in the nuclear density, but due to the large nucleus/electron mass ratio the electron density radius is much larger than the nuclear density radius.

An important conclusion that can be drawn from the present calculations concerns the relation between the size of the ECG basis set, the strategy for the basis set optimization, and total variational energy. The results show that it is possible to obtain a very compact ECG basis set and a very accurate energy if, in the process of growing the basis set, only a few functions are added to the set at a time and, after the addition, the whole basis set is reoptimized several times with a tight optimization threshold. The total nonrelativistic energies obtained is this work for all four lowest  $1S$  states of beryllium atom are better than obtained previously and represent new benchmark values. As this atom becomes somewhat of a model for testing new methods for atomic calculations, improved results such as those obtained in the present work, may provide a useful reference.

## ACKNOWLEDGMENTS

This work has been partially supported by the Ministry of Education and Science of Kazakhstan (state-targeted program BR05236454 “Center of Excellence for Fundamental and Applied Physics”) as well as Nazarbayev University faculty development grant (090118FD5345).

- 
- [1] E. C. Cook, A. D. Vira, C. Patterson, E. Livernois, and W. D. Williams, *Phys. Rev. Lett.* **121**, 053001 (2018).
- [2] S. F. Boys and J. E. Lennard-Jones, *Proc. R. Soc. London, Ser. A* **217**, 136 (1953).
- [3] R. E. Watson, *Phys. Rev.* **119**, 170 (1960).
- [4] A. W. Weiss, *Phys. Rev.* **122**, 1826 (1961).
- [5] H. P. Kelly, *Phys. Rev.* **131**, 684 (1963).
- [6] L. Szasz and J. Byrne, *Phys. Rev.* **158**, 34 (1967).
- [7] R. F. Gentner and E. A. Burke, *Phys. Rev.* **176**, 63 (1968).
- [8] C. F. Bunge, *Phys. Rev.* **168**, 92 (1968).
- [9] J. S. Sims and S. Hagstrom, *Phys. Rev. A* **4**, 908 (1971).
- [10] C. F. Fischer and K. M. S. Saxena, *Phys. Rev. A* **9**, 1498 (1974).
- [11] C. F. Bunge, *Phys. Rev. A* **14**, 1965 (1976).
- [12] L. Adamowicz and A. J. Sadlej, *Chem. Phys. Lett.* **48**, 305 (1977).
- [13] S. A. Alexander, H. J. Monkhorst, and K. Szalewicz, *J. Chem. Phys.* **89**, 355 (1988).
- [14] A.-M. Mårtensson-Pendrill, S. A. Alexander, L. Adamowicz, N. Oliphant, J. Olsen, P. Öster, H. M. Quiney, S. Salomonson, and D. Sundholm, *Phys. Rev. A* **43**, 3355 (1991).
- [15] E. R. Davidson, S. A. Hagstrom, S. J. Chakravorty, V. M. Umar, and C. F. Fischer, *Phys. Rev. A* **44**, 7071 (1991).
- [16] C. F. Fischer, *J. Phys. B* **26**, 855 (1993).
- [17] S. J. Chakravorty, S. R. Gwaltney, E. R. Davidson, F. A. Parpia, and C. F. Fischer, *Phys. Rev. A* **47**, 3649 (1993).
- [18] J. Komasa, W. Cencek, and J. Rychlewski, *Phys. Rev. A* **52**, 4500 (1995).
- [19] O. Jitrik and C. F. Bunge, *Phys. Rev. A* **56**, 2614 (1997).
- [20] H. K. G. Büsse and A. Lüchow, *Int. J. Quantum Chem.* **66**, 241 (1998).
- [21] C. F. Fischer and G. Tachiev, *At. Data Nucl. Data Tables* **87**, 1 (2004).
- [22] K. Pachucki and J. Komasa, *Phys. Rev. Lett.* **92**, 213001 (2004).

- (2004).
- [23] K. Pachucki and J. Komasa, *Phys. Rev. A* **73**, 052502 (2006).
- [24] S. Verdebout, P. Jönsson, G. Gaigalas, M. Godefroid, and C. F. Fischer, *J. Phys. B* **43**, 074017 (2010).
- [25] C. F. Bunge, *Theor. Chem. Acc.* **126**, 139 (2010).
- [26] J. S. Sims and S. A. Hagstrom, *Phys. Rev. A* **83**, 032518 (2011).
- [27] J. S. Sims and S. A. Hagstrom, *J. Chem. Phys.* **140**, 224312 (2014).
- [28] M. Przybytek and M. Lesiuk, *Phys. Rev. A* **98**, 062507 (2018).
- [29] M. Puchalski, K. Pachucki, and J. Komasa, *Phys. Rev. A* **89**, 012506 (2014).
- [30] M. Puchalski, J. Komasa, and K. Pachucki, *Phys. Rev. A* **87**, 030502 (2013).
- [31] M. Stanke, J. Komasa, S. Bubin, and L. Adamowicz, *Phys. Rev. A* **80**, 022514 (2009).
- [32] S. Bubin and L. Adamowicz, *Phys. Rev. Lett.* **118**, 043001 (2017).
- [33] R. J. Drachman, *J. Phys. B* **14**, 2733 (1981).
- [34] K. Pachucki, W. Cencek, and J. Komasa, *J. Chem. Phys.* **122**, 184101 (2005).
- [35] S. Bubin, M. Pavanello, W.-C. Tung, K. L. Sharkey, and L. Adamowicz, *Chem. Rev.* **113**, 36 (2013).
- [36] S. Bubin and L. Adamowicz, *Phys. Rev. A* **79**, 022501 (2009).
- [37] S. Bubin and L. Adamowicz, *J. Chem. Phys.* **128**, 114107 (2008).
- [38] M. Hamermesh, *Group Theory and Its Application to Physical Problems* (Addison-Wesley, Reading, MA, 1962).
- [39] W. E. Caswell and G. P. Lepage, *Phys. Lett. B* **167**, 437 (1986).
- [40] K. Pachucki, *Phys. Rev. A* **56**, 297 (1997).
- [41] H. A. Bethe and E. E. Salpeter, *Quantum Mechanics of One- and Two-Electron Atoms* (Plenum, New York, 1977).
- [42] A. I. Akhiezer and V. B. Berestetskii, *Quantum Electrodynamics* (John Wiley & Sons, New York, 1965).
- [43] H. Araki, *Prog. Theor. Phys.* **17**, 619 (1957).
- [44] J. Sucher, *Phys. Rev.* **109**, 1010 (1958).
- [45] P. K. Kabir and E. E. Salpeter, *Phys. Rev.* **108**, 1256 (1957).
- [46] Z.-C. Yan and G. W. F. Drake, *Phys. Rev. Lett.* **81**, 774 (1998).
- [47] K. Pachucki, *J. Phys. B* **31**, 5123 (1998).
- [48] K. Pachucki, *Phys. Rev. A* **74**, 022512 (2006).
- [49] H. Nakatsuji, H. Nakashima, Y. Kurokawa, and A. Ishikawa, *Phys. Rev. Lett.* **99**, 240402 (2007).
- [50] P. Seth, P. L. Ríos, and R. J. Needs, *J. Chem. Phys.* **134**, 084105 (2011).
- [51] A. Kramida and W. C. Martin, *J. Phys. Chem. Ref. Data* **26**, 1185 (1997).
- [52] L. Johansson, *Ark. Fys.* **23**, 119 (1963).